

Vibrations and electronic states in a model amorphous metal*

J. J. Rehr and R. Alben[†]

Department of Physics, University of Washington, Seattle, Washington 98195

(Received 19 April 1977)

Calculations are presented of the electronic and vibrational properties of a periodic, 500-atom unit cell model of the structure of an amorphous metal. We treat both the effects of *topological* and *quantitative* disorder, the latter being due to variations of interatomic force constants or hopping matrix elements. Topological structure in the model is characterized in terms of the radial distribution function, near-neighbor ring statistics, and the static scattering function $I(Q)$. Calculations are presented of the vibrational density of states, the neutron scattering law $S(Q, \omega)$, and the electronic density of states. In these calculations, the structural disorder is treated exactly, within the framework of simplified models retaining only first-nearest-neighbor interactions. Despite these approximations we expect that the vibrational structure will accurately characterize experimental neutron scattering results in amorphous metals such as PdSi alloys. We find that topological disorder alone does not destroy gross features in the density of states. However, quantitative disorder broadens the electronic spectra and washes out structure in the vibrational density of states almost completely.

I. INTRODUCTION

There has been considerable progress in recent years in understanding vibrational effects^{1,2} and electronic spectra³⁻⁵ in amorphous semiconductors and oxide glasses. Far less attention has been directed at these problems in amorphous metals.⁶⁻⁸ In this paper we consider such effects in a periodic, 500-atom unit cell, structural model of an amorphous metal. We present calculations of the vibrational density of states, the scattering law $S(Q, \omega)$ for vibrations, and the density of states for a simple electronic Hamiltonian. We also discuss the topological properties of this model. We emphasize the results for vibrational properties since we believe our interaction potential is sufficiently realistic that the theoretical results can be compared directly with proposed neutron scattering experiments.⁹ The electronic calculations deal with a one-band Hamiltonian with varying hopping matrix elements. These results are useful in characterizing effects of "topological" and "quantitative," disorder on the electronic spectra. However they are only a first step toward understanding realistic models for *d*-band metals.

In amorphous metals, as in other amorphous materials, there is no conserved crystal momentum to simplify the description of the vibrational and electronic states. Thus, even the simplest models with a harmonic potential or a one-electron Hamiltonian pose difficult theoretical questions. The origin of the difficulty is in the disordered nature of the atomic environments. In amorphous metals, as in semiconductors, it appears to be a good first approximation to focus on the strong near-neighbor interactions. For these interactions the disorder

has two distinct aspects. First there is "topological disorder" which is associated with the absence of a large-scale, repeating lattice and manifested by the variation in the numbers of closed rings of bonds for each site. Second, there is "quantitative disorder," associated with the variations in the interaction between pairs of neighboring atoms due to variations in their separation distances. In amorphous semiconductors the near-neighbor distances do not vary appreciably so it is often valid simply to neglect quantitative disorder. By contrast, in amorphous metals there is good evidence for a spread of about 15% in near-neighbor distances,¹⁰ so considerable effects of quantitative disorder might be anticipated.

We are aware of two previous studies of vibrations in models which can be interpreted as representing amorphous metals. In one study von Heimendahl and Thorpe⁶ considered the effect of topological disorder alone. They concluded that the vibrational densities of states in real amorphous metals should be similar to those of fcc and hcp materials, and in particular should have two peaks associated, respectively, with transverse- and longitudinal-type modes. In the second study, Rahman *et al.*¹¹ considered the dynamics of a "Lennard-Jones glass," in which both topological and quantitative disorder were treated together. They found an essentially featureless density of states. They also calculated longitudinal and transverse scattering functions for relatively small wave vector Q . There has also been some recent work on the structure of the electronic *d* bands in amorphous metals.⁷ The emphasis of that study concerns the effects of topological disorder in liquid and amorphous metals.

In the present study we consider successively both the effects of topological and quantitative disorder. We assume simple first-nearest-neighbor interaction Hamiltonians, with varying amounts of quantitative disorder spanning values which can reasonably be expected for real amorphous metals. We obtain results, particularly for vibrations, which we can confidently apply to real amorphous metals. In our calculations, we make use of a finite (500 atom) model with periodic boundary conditions constructed by Rahman *et al.*¹¹ This model has structural features very similar to models for amorphous or liquid metals, though it was originally obtained as a representation of a Lennard-Jones glass.

The principal conclusions of this study are as follows. We find that for vibrations in real amorphous metals, the quantitative disorder should wash out the two peaks in vibrational density of states left by the topological disorder alone. However, the quantitative disorder does not significantly affect the rotonlike behavior found in a study with topological disorder only.⁶ Although our calculation was made for a one-component model, this conclusion should apply for the low-frequency part of the scattering in the amorphous alloy $\text{Pd}_{80}\text{Si}_{20}$, where the modes associated with the relatively light Si atoms should be confined to frequencies above about 200 cm^{-1} . From the electronic calculations we would expect that the quantitative disorder expected for real amorphous metals has a relatively modest ($\sim 1 \text{ eV}$) broadening effect on the spectrum. This reflects a somewhat smaller variation in the near-neighbor interaction compared to that in the vibrational case.

The paper is divided into five sections. In Sec. II we describe the 500-atom model amorphous structure, and we present results for the radial distribution function, the static scattering function $I(Q)$, and the distribution of three- and four-membered rings of near-neighbor bonds. In Sec. III we briefly review the equation-of-motion method for obtaining spectra for large finite models. In Sec. IV we present our results for vibrations. We discuss in detail the adequacy of the nearest-neighbor, central-force model in crystalline transition metals and, using the measured anharmonic properties of such crystals, we obtain quantitatively the force-constant disorder appropriate for the amorphous structure. We also consider the behavior of $S(Q, \omega)$, in the vicinity of the first peak in $I(Q)$, and we find a broad rotonlike feature. Finally in Sec. V we calculate the density of states for simple electronic Hamiltonians, the quantitative disorder in the hopping matrix elements being estimated from band calculations in transition metals.

II. MODEL

The model amorphous structure used in our studies is a *periodic*, 500-atom unit cell structure, originally developed by Rahman *et al.*¹¹ to investigate properties of a Lennard-Jones glass. As discussed below, however, its properties are well suited for the study of an amorphous metal.¹⁰ This model was constructed using molecular-dynamics techniques and has periodic boundary conditions in a cube of side $L = 8.07\sigma$ (density $N/V = 0.95/\sigma^3$). In our calculations of electronic and vibrational properties, therefore, we treat this system as a finite, 500-atom cluster with periodic boundary conditions. In this section we characterize properties of this model in terms of its radial distribution function, the static scattering function $I(Q)$, and near-neighbor ring statistics.

A. Radial distribution function

The radial distribution function $J(r)$ for the 500-atom model is defined as

$$J(r) = \frac{1}{N} \sum_{i,j} \delta(r - |\vec{r}_i - \vec{r}_j|_L). \quad (1)$$

Here $|\vec{r}_i - \vec{r}_j|_L$ is the distance between sites i and j , modulo an appropriate translation in the cubic unit cell. Essentially $J(r)$ gives the average number of particles per unit shell thickness a distance r from a given site, i.e., $J(r) = 4\pi r^2 n(r)$, where $n(r)$ is the pair distribution function. We have plotted $J(r)$ for the 500-atom model in dimensionless units $\hat{J}(r/\sigma) = \sigma J(r)$ in Fig. 1. For comparison we have also plotted $\hat{J}(r/\sigma)$ for a uniform mass distribution and for a "thermally disordered" FCC structure¹² of the same density.

The spread of nearest-neighbor distances (12%) is similar to that expected for models of amor-

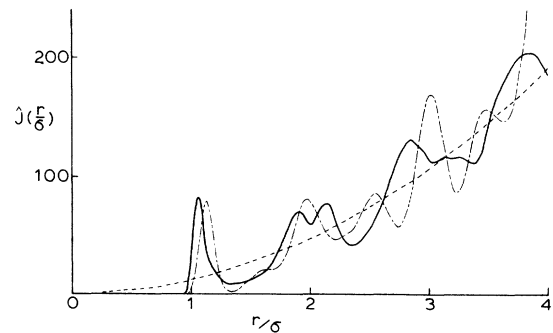


FIG. 1. Radial distribution function (in dimensionless units) for the 500-atom amorphous structure (solid line), a "thermally disordered" fcc structure (Ref. 12) (long dashes), and a uniform mass distribution (short dashes).

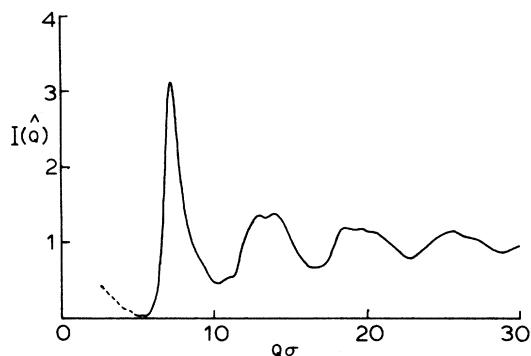


FIG. 2. Static scattering function for the 500-atom amorphous structure.

phous and liquid metals (15%). Also the split second-neighbor peak, with peak distances in the ratio of $2/\sqrt{3}$; and the rather long-range oscillations in $J(r)$ are features typical of amorphous structures described in the literature.^{10,13} Note however that there is little resemblance to the structure in the fcc crystal. The difference in the average first-neighbor distances (1.06σ for the 500-atom amorphous model; 1.14σ , FCC) indicates that the amorphous structure is substantially more loosely packed than are fcc crystals. The hard-sphere diameter 1.06σ at density $0.95/\sigma^3$ corresponds to a packing fraction of 0.60 (compared to 0.74 for fcc), which is comparable to that reported for other models.¹³

B. Scattering function $I(Q)$

The static scattering function $I(Q)$ is proportional to the three-dimensional Fourier transform of the pair distribution function $n(r)$; for an amorphous structure this reduces, on averaging, to

$$I(Q) = \int_0^\infty dr J(r) \frac{\sin Qr}{Qr}, \quad (2)$$

which we have plotted in Fig. 2, in dimensionless units, $\hat{Q} = Q\sigma$. The sharp peak reflects the presence of rather long-range oscillations in $J(r)$.

C. Coordination number and ring statistics

Electronic and vibrational properties (Secs. IV and V) are strongly coupled to the local distribution of bonds and their connectivity in a given structure. Here we discuss the average coordination number and the distribution of m -membered "rings," each "ring" being a closed, self-avoiding path of n -bond steps.

1. Coordination number

Since the dividing line between first and second neighbors in an amorphous metal structure is not

precisely defined, the coordination number z does not have a precise meaning. We shall consider two atoms to be *first*-nearest neighbors if their separation (modulo an appropriate cubic translation) is less than 1.30σ . This distance corresponds to a pronounced minimum in $J(r)$ (Fig. 1), so that a somewhat different division criterion would not significantly change our results. This criterion leads to an average coordination number of 12.048 ± 0.67 (the error is \pm one standard deviation). This value is rather close to that in close-packed structures (12 for fcc), but slightly larger than that reported for the models of Sadoc ($Z = 11$) and Bletry ($Z = 11.5$) used in the study of Gaspard.⁷

2. Three-membered rings

The total number of *distinct* three-membered rings for the 500-atom amorphous model is 4155, somewhat larger than that in a $5 \times 5 \times 5$, 500-atom fcc structure (4000 rings). This corresponds to an average of 49.86 ± 6.4 rings intersecting a given site, compared to 48 for the fcc.

3. Four-membered rings; elemental rings

The total number of distinct four-membered rings in the 500-atom amorphous structure is 17 140, somewhat larger than the number 16 500 counted for a 500-atom $5 \times 5 \times 5$ fcc structure. This corresponds to an average of 274.24 ± 40 rings intersecting a given site, compared with 264 for the fcc.

The numbers mentioned so far might suggest that the local connectivity properties of the 500-atom model do not differ substantially from those of close-packed fcc crystals. This is misleading. The two structures differ significantly in the number of "elemental" four-membered rings, i.e., those four-membered rings which cannot be split (by adding a bond) into two three-membered rings. The 500-atom amorphous model has only 1063 such elemental rings; they are broadly distributed with an average of 17.00 ± 6.5 such rings per site, compared with 1500 such rings or 24 per site for the fcc structure. Furthermore the number of such rings at a given site is strongly anticorrelated with the number of three-membered rings. This suggests that the reduction in such four-membered rings partly accounts for the increased number of three-membered rings.

III. EQUATION-OF-MOTION METHOD

In this section we outline briefly the equation-of-motion method used in calculating the electronic and vibrational densities of states. For more detailed accounts of this method the reader is re-

ferred to the papers of Alben *et al.*¹⁴ (electronic problem) and Beeman and Alben¹⁵ (vibrational). This method has several advantages compared with other means of calculating densities of states. Since matrix diagonalization is not required, the method is quite efficient in dealing even with very large structures containing thousands of atoms.

A. Electronic density of states—one-band model

The equation of motion method is based on the following integral expression for the density of electronic states projected onto a given initial state of the system $|\psi\rangle = \sum_i \psi_i(0)|i\rangle$:

$$g(E) = \text{Re} \frac{1}{\pi} \int_0^T \sum_i \psi_i^*(0) \psi_i(t) e^{i\omega t - \lambda t^2} dt. \quad (3)$$

Here $E = \hbar\omega$, and $\psi_i(t)$ is a solution to the time-dependent Schrödinger equation

$$i \frac{\partial \psi_i}{\partial t} = \sum_j \frac{H_{ij}}{\hbar} \psi_j, \quad (4)$$

subject to a fixed set of initial conditions $\psi_i(0)$, which defines the initial state, and normalization, $\sum_i |\psi_i|^2 = 1$. Equation (3) is evaluated by Simpson's rule with $\psi_i(t)$ determined by integrating the differential equation (4) numerically, using a simple, two-step difference equation approximation.

The cutoff parameters T and λ in Eq. (3) lead to a finite resolution function $\Delta(\omega)$ in the density of states (which reduces to a δ function in the limits $T \rightarrow \infty$, $\lambda \rightarrow 0$). This resolution function conveniently smooths the purely discrete spectrum of a finite model. The form of $\Delta(\omega)$ may be obtained by evaluating Eq. (3) formally in terms of the eigenstates $\phi_i^{(k)}$ of the Hamiltonian H_{ij} with energies $\hbar\omega_k$:

$$g(E) = \sum_k \left| \sum_i \psi_i^*(0) \phi_i^{(k)} \right|^2 \Delta(\omega - \omega_k), \quad (5)$$

where

$$\Delta(\omega) = \frac{1}{\pi} \int_0^T \cos \omega t e^{-\lambda t^2} dt. \quad (6)$$

In practice the resolution width in $\Delta(\omega)$ is typically 5% of the bandwidth, and the value $\lambda = -3/T$ leads to a small oscillatory tail in $\Delta(\omega)$. The numerical integration requires typically 100 steps.

In principle the total density of states is obtained by evaluating Eq. (3) for a complete set of initial states, for example the states defined by the initial conditions $\{\psi_i(0) = 1, \psi_j(0) = 0, j \neq i\}$. There are 500 such states for the 500-atom amorphous model. In practice it is far more efficient to evaluate Eq. (3) for a small number of initial states which more or less uniformly sample the full spectrum. A convenient set of states for this purpose are those

defined by the initial conditions $\psi_i(0) = e^{i\mu_i}$, where μ_i are random phases uniformly distributed in the interval $(0, 2\pi)$.

Fluctuations in the occupation probability of a given eigenstate $\phi_i^{(k)}$ are largely averaged out by the resolution function $\Delta(\omega)$. However, this procedure does introduce a small statistical error in to the calculated density of states, in addition to that from the resolution width, finite size effects, and approximations inherent in the numerical integrations.

B. Vibrational density of states

The calculation of the vibrational spectra is analogous to the procedure for the electronic spectra, except that three states per site must be considered, and the equation of motion is slightly different. In this case the density of vibrational states is given by

$$g(\omega) = \text{Re} \frac{1}{\pi} \int_0^T \sum_{i,\alpha} x_{i\alpha}^0 x_{i\alpha}(t) e^{i\omega t - \lambda t^2} dt. \quad (7)$$

Here $x_{i\alpha}(t)$ is the α -component of the displacement of the i th ion, with mass m_i . These displacements satisfy the equation of motion

$$m_i \frac{d^2 x_{i\alpha}}{dt^2} = \sum_{j,B} V_{i\alpha,jB} x_{jB}, \quad (8)$$

subject to the initial conditions with specified $x_{i\alpha}^0 = x_{i\alpha}(0)$, and $\dot{x}_{i\alpha}(0) = 0$. Equations (7) and (8) are evaluated numerically, using techniques similar to those used in the electronic case. Similarly the total density of states is obtained statistically, using initial states with a given set of random phases, $x_{i\alpha}^0 = \cos \mu_{i\alpha}$.

IV. VIBRATIONS

A. Elastic energy

A calculation of the vibrational properties of amorphous metals has two main ingredients. The first is a model for the equilibrium structure, for which we use the 500-atom amorphous model described in Sec. II. The second ingredient is a form for the elastic energy. This must be simple and free of undetermined parameters, but accurate enough to describe features of the spectra semi-quantitatively. We thus assume a restricted harmonic form for the energy with near-neighbor central forces, whose distance dependence is estimated from the anharmonic behavior of crystalline materials. The specific form of the energy is that of the Born central force

$$V = \frac{1}{2} \sum_{ij} \alpha_{ij} [(\vec{u}_i - \vec{u}_j) \cdot \hat{r}_{ij}]^2, \quad (9)$$

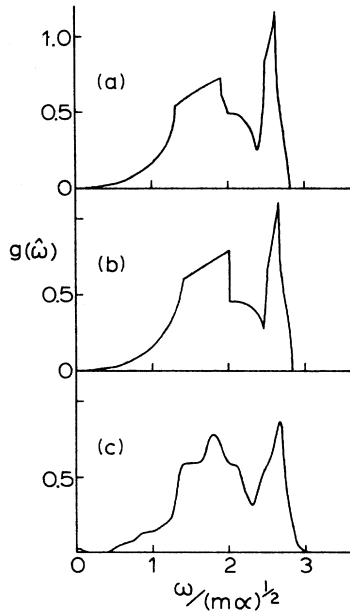


FIG. 3. Vibrational density of states for (a) Cu, 18-parameter fit; (b) Cu, first-nearest-neighbor interaction only; (c) 480-atom $4 \times 5 \times 6$ fcc model.

where the sum is over "nearest-neighbor" pairs of atoms i and j (as defined in Sec. III C), α_{ij} is the force constant for the given pair of atoms, \hat{r}_{ij} is the unit vector from i to j , and \vec{u}_i the displacement from equilibrium.

The adequacy of such a near-neighbor central-force model for the overall behavior of the vibrations can be tested against results for force-constant models with many free parameters chosen to fit the phonon dispersion in fcc crystals. Such a test is shown in Figs. 3(a) and 3(b), where the phonon density of states of copper, calculated from an 18-parameter force-constant model,¹⁶ is compared with the result obtained with a single first-nearest-neighbor force constant¹⁷ ($\alpha = 27.9$ N/m). Here $\hat{\omega} = \omega/(\alpha m)^{1/2}$ is a dimensionless frequency. The agreement is seen to be excellent. In Fig. 3(c) is a plot of the vibrational density of states for a periodic, 480-atom $4 \times 5 \times 6$ fcc model as calculated by the method of Sec. III with a broadening width (full width at half maximum) $\Delta \hat{\omega} = 0.15$. This last result indicates that the overall form of the density of states for crystalline Cu can be reasonably well reproduced by a nearest-neighbor central-force elastic energy applied to a model with about 500 atoms.

In order to apply the form of V to the 500-atom disordered model, we must account for the variation of the force constants with bond length. We do this by examining experimental results for the anharmonic properties of crystalline metals. Ideally

we would like to have results for the variation of the full spectrum of phonon frequencies with bond distance, but these are not available. The more readily available anharmonic information comes from elastic constants. In the table below we show the measured elastic constants for copper¹⁸ compared with those due to the nearest-neighbor central-force alone.¹⁶

	Experiment (N/m ²)	Nearest neighbor
C_{11}	1.765×10^{11}	1.544×10^{11}
C_{12}	1.252×10^{11}	0.772×10^{11}
C_{44}	0.818×10^{11}	0.772×10^{11}

It is seen that, despite excellent agreement with the near-neighbor central-force model for the overall phonon spectrum, the agreement for the elastic constants is only approximate. This is not surprising, since contributions to the elastic constants are weighted by the square of the interaction range. Thus, we can only roughly approximate the behavior of the nearest-neighbor force from variations of the elastic constants. In this spirit, we consider two results which would roughly determine the force-constant variation if near-neighbor central forces were dominant.

We define a dimensionless anharmonicity parameter A as

$$A = -\frac{r_0}{\alpha} \frac{d\alpha}{dr} = -\frac{r_0}{w''(r)} w'''(r), \quad (10)$$

where $w(r)$ is the potential between a pair of interacting atoms at separation r_0 . For near-neighbor central forces A is related to the pressure derivative of the bulk modulus¹⁸:

$$A = 3 \left(\frac{\partial B}{\partial p} - 1 \right). \quad (11)$$

Using the measured value¹⁸ $\partial B/\partial p = 5.59$, we obtain $A = 13.8$. The second way of getting A is from the third-order elastic constant¹⁹ C_{111} :

$$A = -2(C_{111}/C_{11}) - 3. \quad (12)$$

Using the value $C_{111} = -13.9 \times 10^{11}$ N/m², we obtain $A = 12.8$. Of course many other combinations of third-order elastic properties could be used to estimate A , but the result $A \sim 13$ is typical and will be assumed below to be characteristic of copper and other d -electron metals.

It might be expected that information about the anharmonicity could also be obtained from the Grüneisen parameter. In the simple Grüneisen theory, the mode frequencies depend only on the volume, and it can readily be seen that $A = 6\gamma$ for the near-neighbor model. The Grüneisen parameter γ for copper²⁰ is about 2.0, giving $A = 12$.

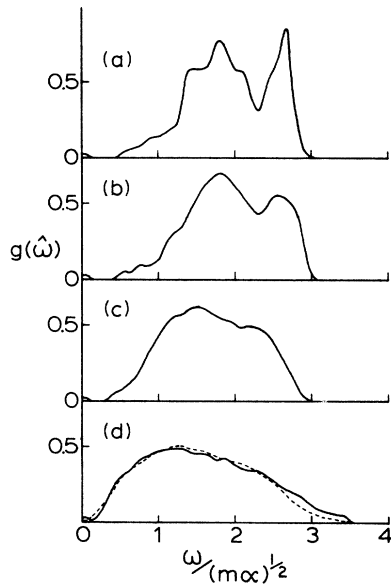


FIG. 4. Effect of disorder on the vibrational density of states: (a) 480-atom fcc model, (b)–(d) 500-atom amorphous model with (b) constant force-constants ($A = 0$), (c) a Morse potential ($A = 9.8$), and (d) a Lennard-Jones potential ($A = 19.5$). The dashed curve in (d) is the result of Ref. 11.

Although this number agrees with the above results, measurements of the temperature behavior of the phonon frequencies¹⁶ indicate that this simple theory does not apply very well to copper, so we base our value for A on the elastic constant results.

Given a value for the anharmonicity A , we can examine various forms for the interatomic potential and choose one which will approximately reproduce the force-constant variation with bond length. In our numerical calculations we have considered three forms for the interaction potential: (i) The first is a potential with constant curvature, for which $A = 0$ and the force constants are taken to be the same for all atoms close enough to be considered nearest neighbors. (ii) The second is a Morse potential, with parameters as proposed by Girifalco and Weizer,²¹ and the nearest-neighbor distance for the fcc structure is taken to be 1.1σ . For this potential A has a somewhat low value of 9.8, and the force constant varies by a factor of 2.43 over distances in the near-neighbor peak (half-maximum to half-maximum) of the radial distribution function (RDF). (iii) The third potential is the Lennard-Jones potential used by Rahman *et al.*¹¹ in their molecular-dynamics calculations of the 500-atom amorphous structure. For this potential $A = 19.5$, and the force constant varies in strength by a factor of 7.0 over the near-neighbor peak. The

desired potential with $A = 13$ is intermediate between (ii) and (iii) but somewhat closer to (ii).

Results for the vibrational density of states for the 500-atom model for these three potentials are shown in Figs. 4(b)–4(d), respectively. In each case the frequency is normalized by that corresponding to the value of $\alpha(r)$ at $r = 1.1\sigma$, which is the average nearest-neighbor distance, $\hat{\omega} = \omega / [m\alpha(1.1\sigma)]^{1/2}$. (If the results were normalized by the value of α at 1.07σ , the distance corresponding to the peak in the RDF, the spectra for the 500-atom disordered model would be shifted to lower frequency.) For comparison, the result for the periodic, 480-atom $4 \times 5 \times 6$ fcc model, calculated with the same resolution, is given in Fig. 4(a). In Fig. 4(d), we also include the molecular-dynamics result of Ref. 11 for the Lennard-Jones potential without the cutoff used in our work. The interpretation of these results is that the two-peaked form of the crystalline density of states is not removed by topological disorder, in agreement with previous work.⁶ However even for a somewhat smaller force-constant variation than that expected for real amorphous metals [Fig. 4(c)], the spectrum is very much washed out.

The neutron scattering law $S(Q, \omega)$ is defined by the relation

$$S(Q, \omega) = \frac{1}{\pi} \int_0^\infty \sum_i \vec{Q} \cdot \vec{u}_i(0) e^{i\vec{Q} \cdot \vec{R}_i} \times \sum_j \vec{Q} \cdot \vec{u}_j(t) e^{-i\vec{Q} \cdot \vec{R}_j} \cos \omega t dt. \quad (13)$$

Results for a normalized $S(Q, \omega)$,

$$\hat{S}(\hat{Q}, \hat{\omega}) = S(Q, \omega) M \omega / Q^2 [n(\hbar\omega/kT) + 1],$$

are plotted in dimensionless variables [$\hat{Q} = Q\sigma$; $\hat{\omega} = \omega/(m\alpha)^{1/2}$] in Fig. 5, for the Morse function interatomic potential [Fig. 4(c)]. The values of Q range from a small wave vector, for which a sharp longitudinal acoustical mode is seen, to a value beyond the first peak in the static structure function $I(Q)$ (see Fig. 2).

The behavior in the vicinity of the strong first peak in $I(Q)$ at $Q\sigma = 7.21$ can be described as “rotonlike”; as Q increases there is a minimum in the energy corresponding to the maximum scattering. However the effect here is rather different than the roton excitation in superfluid ^4He . Here, the scattering at low energy is enhanced for Q near peaks in $I(Q)$, since at these points the structure can statically absorb momentum, allowing long-wavelength low-energy excitations to contribute to the scattering.¹ The case treated has somewhat less quantitative disorder than we estimated for real amorphous metals. However the rotonlike effect in Fig. 5 is not much different from that found by

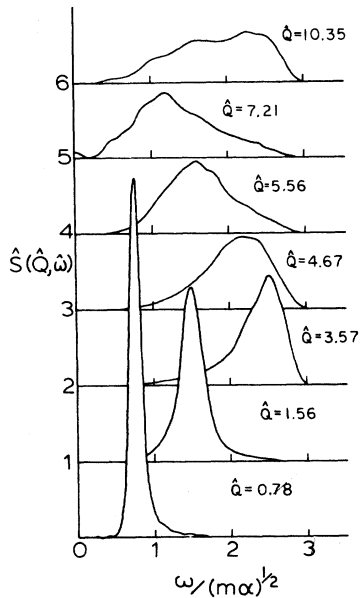


FIG. 5. Normalized (see text) neutron scattering law $\hat{S}(\hat{Q}, \hat{\omega})$ for the 500-atom amorphous model calculated using a Morse potential ($A = 9.8$), illustrating a "roton-like" behavior.

von Heimendahl for case of constant near-neighbor forces. Thus this roton effect does not seem to be very sensitive to quantitative disorder, and it seems likely that it would be found in real materials.

V. ELECTRONIC PROPERTIES

In this section we describe the electronic properties of the 500-atom amorphous model with a tight-binding one-band Hamiltonian. While this model is highly simplified it serves to illustrate the effects of topological and quantitative disorder in the density of states, without the complexity of a calculation with five d -orbitals per site. Otherwise the spectra for this model is largely unrealistic.

To study the effects of *quantitative* disorder, we have adopted a simple exponential form for the hopping matrix element similar to that used in studies of liquid metals²²:

$$H_{ij} = \begin{cases} V e^{-\alpha(r_{ij}-r_0)/r_0}, & r_{ij} \leq 1.3\sigma, \\ 0, & \text{otherwise.} \end{cases} \quad (14)$$

The criterion $r_{ij} < 1.3\sigma$ corresponds to our definition of first "nearest neighbors" (Sec. II). To study *topological* disorder alone, for which H_{ij} is constant, we set $\alpha = 0$. Densities of states $g(E)$ were calculated using the equation-of-motion method (Sec. III) for several values of α . Effects of finite

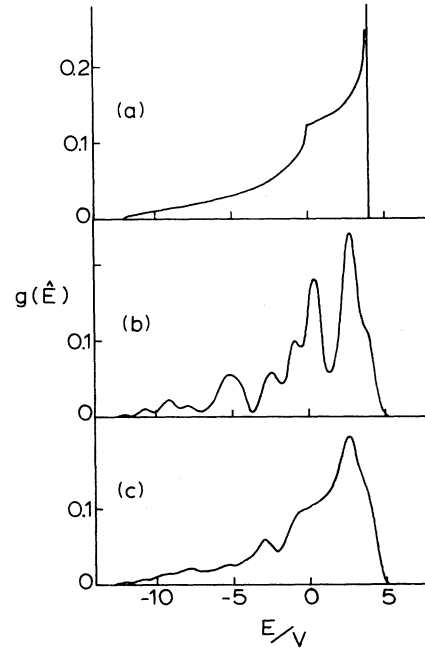


FIG. 6. Electronic density of states for one-band fcc models: (a) exact result (Ref. 23); (b) 500 atom $5 \times 5 \times 5$ fcc model; and (c) 480-atom $4 \times 5 \times 6$ fcc model.

model size were investigated by comparing the results with those of two fcc structures with nearest-neighbor, tight-binding Hamiltonians (with hopping matrix element V): a periodic 500-atom $5 \times 5 \times 5$

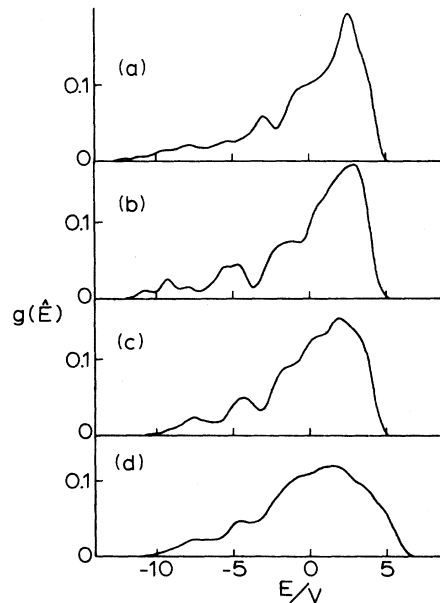


FIG. 7. Effect of disorder on the electronic density of states: (a) 480-atom fcc structure, (b)–(d) 500-atom amorphous structure with (b) no disorder, (c) $\alpha = 7.5$, and (d) $\alpha = 15$ (see text).

model, and a periodic, 480-atom $4 \times 5 \times 6$ model. All calculations were performed with identical resolution functions.

In Fig. 6 we illustrate the effects of finite size, shape, and resolution in the equation-of-motion method by presenting calculations for these finite fcc crystals. The resolution (full width, half maximum) is 1.0, that is, about 6% of full bandwidth. Figure 6(a) shows the density of states of a regular fcc crystal with this tight-binding Hamiltonian,²³ plotted in dimensionless units $\hat{E} = E/V$.

Figure 6(b) shows the density of states for the periodic 500-atom $5 \times 5 \times 5$ fcc structure; and Fig. 6(c), that for the 480-atom $4 \times 5 \times 6$ fcc structure. The ripple in Fig. 6(b) is due to degeneracies arising from cubic symmetry and the small number of modes in the $5 \times 5 \times 5$ crystal. Evidently the less symmetric $4 \times 5 \times 6$ structure has a spectrum which more uniformly covers that in the infinite crystal. However, small finite size effects are still apparent. Note that the band edges are quite close to the values -12 and $+4$ of the infinite crystal.

Figure 7 illustrates the various effects of disorder. In Fig. 7(a), we have reproduced the den-

sity of states for the 480-atom fcc structure for comparison. Figures 7(b)–7(d) correspond to values of α in Eq. (1) of 0, 7.5, and 15, respectively. Note first that topological disorder alone ($\alpha = 0$) smoothes, but does not significantly alter the nature of the density of states. This conclusion is basically consistent with the findings of Gaspard for d bands. The ripple in the low-energy tail can be attributed to finite size effects: We might expect that long-wavelength electronic excitations of our 500-atom models, both fcc and amorphous, will be rather insensitive to structural details. That this is indeed the case may be seen by examining the ripple in low-energy tails in Figs. 6(b) and 7(b). The value $\alpha = 7.5$ is typical of that for the d -orbitals of the transition elements,²² and implies a variation in the hopping matrix element by a factor of 2.46 over the first-neighbor peak in the RDF. Since α corresponds to the anharmonicity A [Eq. (10)], the effect of quantitative disorder on the electronic density of states should be substantially less than in the vibrational case ($A = 12$). This reflects the comparative softness of the electronic interaction compared with that for vibrations.

*Supported in part by Air Force Office of Scientific Research and the NSF.

†Present address: Dept. of Engineering and Applied Science, Yale University, New Haven, Conn. 06520.

¹R. Alben, D. Weaire, J. E. Smith, Jr., and M. H. Brodsky, *Phys. Rev. B* **11**, 2271 (1975).

²R. J. Bell and P. Dean, *Nature* **212**, 1354 (1966).

³D. Weaire and M. F. Thorpe, *Phys. Rev. B* **4**, 2508 (1971).

⁴J. Joannopoulos and M. L. Cohen, in *Solid State Physics*, edited by H. Ehrenreich, F. Seitz, and D. Turnbull (Academic, New York, 1976), Vol. 31, p. 71.

⁵S. Pantelides and W. Harrison, *Phys. Rev. B* **13**, 2667 (1976).

⁶L. V. Heimendahl and M. F. Thorpe, *J. Phys. F* **5**, L87 (1975); M. F. Thorpe, L. V. Heimendahl and R. Alben, in *Proceedings of the Third International Conference*, Campinas, Brasil, edited by M. Balkanski (Halsted, New York, 1976), p. 668; L. V. Heimendahl (unpublished).

⁷J. P. Gaspard, *AIP Conf. Proc.* **31**, 372 (1976); and (to be published).

⁸H. K. Peterson, A. Bansil, and L. Schwartz, *AIP Conf. Proc.* **31**, 378 (1976).

⁹H. Mook (private communication).

¹⁰G. S. Cargill III, in *Solid State Physics*, edited by

H. Ehrenreich, F. Seitz, and D. Turnbull (Academic, New York, 1975), Vol. 30, p. 227.

¹¹A. Rahman, M. J. Mandell, and J. P. McTague, *J. Chem. Phys.* **64**, 1564 (1976).

¹²Gaussian distributions for the interatomic distances are introduced with standard deviations $\delta = 0.6\sigma$ (first-nearest neighbors), and $\delta = 0.12\sigma$ (all successive neighbors.)

¹³J. L. Finney, *Proc. R. Soc. A* **319**, 479 (1970).

¹⁴R. Alben, M. Blume, H. Krakanev, and L. Schwartz, *Phys. Rev. B* **12**, 4090 (1975).

¹⁵D. Beeman and R. Alben, *Adv. Phys.* (to be published).

¹⁶R. M. Nicklow, G. Gilat, H. G. Smith, L. J. Raubheimer, and M. K. Wilkinson, *Phys. Rev.* **164**, 922 (1967).

¹⁷J. C. Wheeler, M. G. Prais, and C. Blumstein, *Phys. Rev. B* **10**, 2429 (1975).

¹⁸W. B. Daniels and C. S. Smith, *Phys. Rev.* **111**, 713 (1958).

¹⁹R. D. Peters, M. A. Breazeale, and V. K. Pare, *Phys. Rev. B* **1**, 3245 (1970).

²⁰J. G. Collins, *Philos. Mag.* **8**, 323 (1963).

²¹L. A. Girifalco and V. G. Weizer, *Phys. Rev.* **114**, 687 (1959).

²²F. Cyrot-Lackmann, *Adv. Phys.* **16**, 393 (1967).

²³R. J. Jelitto, *J. Phys. Chem. Solid* **30**, 609 (1969).